

# The effects of mechanical and hydrothermal aging on microstructure and biaxial flexural strength of an anterior and a posterior monolithic zirconia



Eduardo Mariscal Muñoz<sup>a</sup>, Diogo Longhini<sup>a</sup>, Selma Gutierrez Antonio<sup>b</sup>, Gelson Luis Adabo<sup>a,\*</sup>

<sup>a</sup> Department of Dental Materials and Prosthodontics, Araraquara Dental School, Univ Estadual Paulista—UNESP, São Paulo, Brazil

<sup>b</sup> Department of Physical Chemistry, Araraquara Institute of Chemistry, Univ Estadual Paulista—UNESP, São Paulo, Brazil

## ARTICLE INFO

### Keywords:

Mechanical cycling  
Hydrothermal aging  
Anterior monolithic zirconia  
Posterior monolithic zirconia  
Biaxial flexure strength  
Crystalline phase

## ABSTRACT

**Objectives:** To evaluate the effect of hydrothermal aging (H), mechanical cycling (M), and the combination of hydrothermal plus mechanical cycling (H + M) on biaxial flexural strength (BFS) and microstructure of two monolithic zirconias, indicated for anterior (AMZ) or posterior restorations (PMZ) and a conventional zirconia (IZr).

**Methods:** Disc specimens of each material ( $n = 12$ ) were submitted to: i) H (8 h in autoclave at 134 °C); ii) M ( $10^6$  cycles, at 40% of BFS); and iii) H + M. BFS was measured (ISO-6872) and Weibull modulus ( $m$ ) and the characteristic strength ( $\sigma^0$ ) were calculated. Crystalline phase composition analyzed by XRD, and grain size measured by MEV analysis.

**Results:** XRD analysis showed AMZ was not susceptible to monoclinic transformation in any treatment. Conventional zirconia (IZr) and PMZ had monoclinic transformation only after H and H + M. BFS of AMZ was lower than PMZ and IZr. Cubic phase was found in all conditions for AMZ and IZr, while it was identified in PMZ only after H and H + M. BFS of AMZ was affected by M and H + M. For IZr and PMZ the unique difference detected in BFS was in the comparison of H to M. H treatment induced lower Weibull modulus, but characteristic strength was compatible with the BFS results. AMZ grain size ( $\mu\text{m}^2$ ) was 8.6 times larger than PMZ grains, and 13.6 times larger than IZr grains.

**Conclusions:** AMZ showed the largest mean grain size, had the lowest BFS values, and was affected when mechanical cycling was involved. Monoclinic transformation was not found in any treatment for AMZ, but was found in IZr and PMZ when hydrothermal aging was used alone or when combined with mechanical cycling. PMZ showed similar behavior to the IZr. H induced to higher fracture probability.

**Clinical significance:** Translucent monolithic dental zirconia available on the market may behave differently under simulated oral aging. The relationship between composition and microstructure determines their properties presumably, and clinical performance.

## 1. Introduction

Yttria-stabilized tetragonal zirconia polycrystals (Y-TZP) have been widely used in dentistry for crowns and partial fixed prostheses. Given its high opacity, conventional zirconia demands veneering with feldspathic porcelain, but of significant concern is the relatively high rates of delamination or chipping of porcelain [1]. In order to solve this problem, efforts have been made to develop a monolithic Y-TZP (also known as full-contour Y-TZP) with improved optical properties, which would dispense with the need for porcelain veneers [2]. Nevertheless, monolithic Y-TZP is exposed directly to moisture, body temperature, and mechanical load from chewing, which supposedly makes it more susceptible to degradation.

Optimal mechanical performance of Y-TZP is due to a mechanism that enhances its fracture strength, known as phase transformation toughening [3]. This mechanism, described by Garvie et al. [4], is triggered by superficial stress around microcracks, which induce crystalline phase transformation of metastable Y-TZP grains adjacent to the defect from the tetragonal-to-monoclinic crystal system. A volumetric expansion of the involved grains results from phase transformation, which induces compressive stress on the advancing crack, preventing or slowing down crack propagation [5]. Nevertheless, tetragonal-to-monoclinic phase transformation can also occur spontaneously over time due to body temperature and humidity [6], described as low-temperature degradation (LTD). LTD is a thermodynamic and time-dependent phenomenon that can be triggered by water molecules [3,7]

\* Corresponding author at: Department of Dental Materials and Prosthodontics, Rua Humaitá 1680, Araraquara, 14801-903 São Paulo, Brazil.

E-mail addresses: [adabo@foar.unesp.br](mailto:adabo@foar.unesp.br), [gl.adabo@uol.com.br](mailto:gl.adabo@uol.com.br) (G.L. Adabo).

at a wide temperature range (37–500 °C) by an energy barrier breaking after diffusion of water into the zirconia lattice [3,7,8]. In addition to in-bulk stress augmentation originating from LTD [9], other major drawbacks might occur, such as the worsening of optical properties [10] and an increase of wear rates [11] as a consequence of expanded grains uplifting on the surface.

Monolithic zirconia development is addressed by diminishing the opacity of Y-TZP by means of different strategies to eliminate or decrease light-scattering sources such as sintering additives (typically alumina) [12], reduction of oxygen vacancies, pores and defects, controlled sintering environment (i.e. pressure and temperature) [13], and use of specific dopants [14]. Taking into account that tetragonal zirconia crystal is optically anisotropic, refraction occurs in different crystallographic directions. Thus, the resultant birefringence may be contoured by the development of specific grain sizes [15]. Translucency is dependent on the number of grain boundaries. Y-TZP with small grain size means a greater grain-boundary area, and consequent lower translucency. However, larger tetragonal grains are not desirable because their metastability is weaker, and consequently increases LTD susceptibility [16]. Usually, Y-TZP has grain size in the range of 0.2–0.8 µm, which gives some translucency but only up to 1 mm thickness. On the other hand, it is possible to produce transparent to translucent Y-TZP using a nano-scale grain size (under 100 nm), which is markedly smaller than the wavelength range of visible light (400–700 nm) [15]. Thus, a ray of visible light penetrating the material may not be reflected or refracted but transmitted [2]. As result, the birefringent characteristic of Y-TZP given by the anisotropic nature of zirconia tetragonal crystals orientation [17] is minimized.

Another strategy is the use of fully stabilized zirconia (FSZ), which has improved translucency due to the increase in cubic phase concentration. In contrast to tetragonal grain, scattering is reduced because cubic crystals have an isotropic refractive index. Cubic phase stabilization is achieved by adding yttria in concentrations higher than 8 mol %, while in partially stabilized zirconia (PSZ), tetragonal phase is stabilized with 2–5 mol% yttria content [18]. However, a reduction in mechanical resistance is expected, once it has lost the toughening effect resultant from the tetragonal-to-monoclinic phase transformation.

Thus, different methods of producing translucent Y-TZP are obtained by opposite modifications in composition and microstructure. Monolithic zirconia is relatively recent, and there is little evidence based on clinical assays or in vitro long-term degradation studies, which would show how this different translucent ceramic would behave over time under LTD and mechanical challenges. Hence, the null hypothesis of this study is that the flexural strength and microstructure of two monolithic zirconias (for posterior teeth and for anterior teeth) are not affected by the following accelerated aging methods: mechanical cycling; simulation of LTD by hydrothermal aging; and the combination of mechanical cycling plus hydrothermal aging.

## 2. Materials and methods

The composition of each material is detailed in Table 1. A monolithic zirconia for anterior restorations (AMZ) and one for posterior

**Table 2**  
Two-way ANOVA analysis.

Source	Sum of squares	df	Mean square	F	P value
Material	1707354.536	2	853677.85	103.808	< 0.001
Aging	257583.990	3	85861.330	10.441	< 0.001
Interaction	126868.776	6	21144.796	2.571	0.022
Error	1085519.592	132	8223.633		
Total	44354905.74	144			
Corrected total	3177326.895	143			

restorations (PMZ) were analyzed, a zirconia for infrastructure (IZr) was included as a control group.

### 2.1. Specimen preparation

Commercially available blocks were machined into cylindrical bars, which were sectioned (IsoMet 1000, Buehler, IL, USA/Extex High Concentration, Extex Enfield, CT, USA) under water cooling to obtain disc specimens. Prior to sintering process, specimens were smoothed on both sides using silicon carbide grinding paper (FEPA no. 4000 Struers LaboPol 21, Struers, Rodovre, Denmark) for 30 s using an automatic polisher (Aropol-2 V, Arotec, SP, Brazil) under distilled water cooling, at a rotational speed of 300 rotations per min and pressure of 0.98 N/cm<sup>2</sup>. The specimens were ultrasonically cleaned in distilled water for 15 min and dried for 2 h at 37 °C before sintering in the furnace, InFire HTC speed (Sirona, Salzburg, Austria). The heating and cooling rates were 8 °C/min and the materials were maintained at maximum temperatures for 2 h (anterior monolithic zirconia (AMZ) and posterior monolithic zirconia (PMZ) at 1600 °C, and IZr at 1500 °C). After sintering, the specimens' final dimension (12.0 diameter and 1.2 mm thickness) was accomplished to ISO 6872:2015. Additionally, the specimens were polished using monocrystalline water-based diamond suspension (1 µm for 3 min, and 0.25 µm for 4 min at speed 300 RPM, 0.98 N/cm<sup>2</sup> load – MetaDi, Buehler, IL, USA) in a polisher (Aropol-2 V, Arotec).

### 2.2. Accelerated aging methods

Specimens were artificially aged according to the following treatment groups: I) hydrothermal degradation (H); II) mechanical cyclic load (M); III) mechanical cyclic plus hydrothermal degradation (H + M); IV) non-treated specimens (control group). Hydrothermal degradation was carried-out in an autoclave at 134 °C for 8 h under 0.2 MPa of pressure (AB-25, Phoenix Luferco, SP, Brazil) [19]. Mechanical cyclic loading was applied to the specimens in 10<sup>6</sup> cycles of biaxial bending on a piston and three balls set-up (following ISO 6872:2015 configuration), using a universal cycling machine (Biocycle, Biopdi, SP, Brazil) under distilled water immersion at 37 °C. The cycling load was set at 40% of the mean static resistance, previously obtained from static biaxial flexure test of non-treated materials for each material (n = 12). Cycling load was set to 40% to ensure survival of the specimens. For AMZ the load was set at 350 N; for PMZ 450 N,

**Table 1**  
Basic composition and nomenclature of the materials investigated.

Material	Code	Composition <sup>a</sup>	Fabricant/batch number
High translucency anterior monolithic zirconia	AMZ	< 12% Y <sub>2</sub> O <sub>3</sub> 1% Al <sub>2</sub> O <sub>3</sub> , max. 0.02% SiO <sub>2</sub> , max. 0.01% Fe <sub>2</sub> O <sub>3</sub> , max. 0.04% Na <sub>2</sub> O	Prettau Anterior, Zirkonzahn, Bruneck, Italy/ZB4221B
High translucency posterior monolithic zirconia	PMZ	4–6% Y <sub>2</sub> O <sub>3</sub> , < 1% Al <sub>2</sub> O <sub>3</sub> , max. 0.02% SiO <sub>2</sub> , max. 0.01% Fe <sub>2</sub> O <sub>3</sub> , max. 0.04% Na <sub>2</sub> O	Prettau, Zirkonzahn, Bruneck, Italy/ZB3208A
Zirconium infrastructure ceramic (control)	IZr	4–6% Y <sub>2</sub> O <sub>3</sub> , < 1% Al <sub>2</sub> O <sub>3</sub> , max. 0.02% SiO <sub>2</sub> , max. 0.01% Fe <sub>2</sub> O <sub>3</sub> , max. 0.04% Na <sub>2</sub> O	ICE Zirkon, Zirkonzahn, Bruneck, Italy/ZB4131B

<sup>a</sup> From Sulaiman TA, et al. Impact of gastric acidic challenge on surface topography and optical properties of monolithic zirconia. Dent Mater (2015) <http://dx.doi.org/10.1016/j.dental.2015.09.010>.

**Table 3**  
Mean biaxial flexure strength values (MPa) for the materials after aging.

	IZr	PMZ	AMZ
Non-treated	1048.1 ± 131.3 <sup>Aab</sup>	1162.6 ± 150.3 <sup>Aab</sup>	853.5 ± 123.2 <sup>Ba</sup>
Hydrothermal	1187.2 ± 297.5 <sup>Aa</sup>	1189.3 ± 246.8 <sup>Aa</sup>	721.8 ± 208.7 <sup>Ba</sup>
Mechanical	965.4 ± 106.6 <sup>Ab</sup>	992.0 ± 115.2 <sup>Ab</sup>	552.3 ± 89.2 <sup>Bb</sup>
Hydrothermal & mechanical	1066.7 ± 107.4 <sup>Aab</sup>	1035.1 ± 137.6 <sup>Aab</sup>	531.1 ± 44.2 <sup>Bb</sup>

Different superscript uppercase letters in rows, and lowercase letters in columns indicate significant difference ( $p < 0.05$ , Tukey test,  $n = 12$ ).

**Table 4**  
Weibull Modulus ( $m$ ) and Characteristic Strength (MPa) for the materials after aging.

		Non-treated	Hydrothermal	Mechanical	Hydrothermal & mechanical
IZr	Weibull Modulus	8.11	4.07	9.34	10.33
	Characteristic Strength	1108.63	1303.96	1012.93	1113.62
PMZ	Weibull Modulus	6.97	5.01	8.97	7.87
	Characteristic Strength	1236.78	1287.18	1041.92	1089.28
AMZ	Weibull Modulus	6.95	2.79	6.49	11.86
	Characteristic Strength	906.54	824.84	588.08	553.47

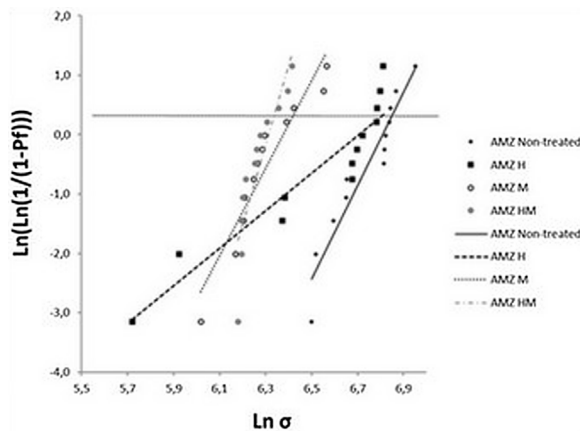


Fig. 1. Weibull analysis plot for AMZ groups.

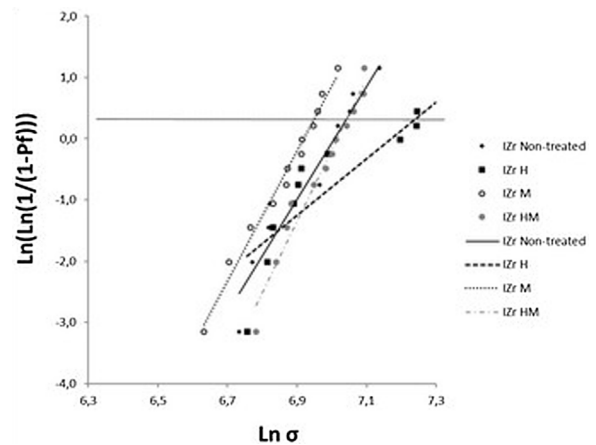


Fig. 3. Weibull analysis plot for IZr groups.

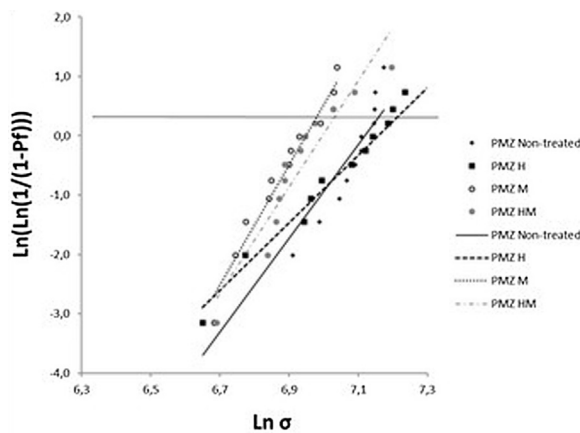


Fig. 2. Weibull analysis plot for PMZ groups.

and for IZr 420 N. Load was applied through stainless steel spherical indenters (8 mm diameter) at 125-ms intervals (4 Hz frequency), simultaneously in 10 specimens. During the cycling process, small pieces (10.0 mm diameter) of transparency acetate film for printing (transparency film CG5000, 3M, MN, USA), were lodged between the specimen surface and the indenter to avoid superficial crack induction. These acetate films were completely flexible to allow a complete force transmission.

### 2.3. Effect of aging processes on biaxial flexure resistance

Biaxial flexure tests were conducted according to ISO 6872:2015 ( $n = 12$ ) in a universal test machine (DL, Emic, PR, Brazil), at a cross head speed of 1 mm/min until failure occurred. The load to failure was registered in N and then calculated in MPa according to the following equation (ISO: 6872:2015):

$$S = -0.2387 \frac{P(X - Y)}{d^2} \quad (1)$$

In which  $S$  represents the maximum tensile stress in MPa,  $P$  is the total load to fracture in Newtons and  $d$  is the specimen thickness (mm).  $X$  and  $Y$  were obtained as follows:

$$X = (1 + \nu) \ln \left( \frac{r_2^2}{r_3^2} \right) + \left[ \frac{(1 - \nu)}{2} \right] \left( \frac{r_2}{r_3} \right)^2$$

$$Y = (1 + \nu) \left[ 1 + \ln \left( \frac{r_2^2}{r_3^2} \right) \right] + (1 - \nu) \left( \frac{r_1}{r_3} \right)^2 \quad (2)$$

Where:  $\nu$  is Poisson's ratio ( $= 0.23$ );  $r_1$  is the radius of support circle,  $r_2$  the radius of loaded area,  $r_3$  the radius of specimen, all of these expressed in millimeters.

### 2.4. Weibull analysis

Weibull regression analysis was performed based on the flexural strength data to determine the Weibull modulus and characteristic strength. The Weibull distribution were calculated according to the

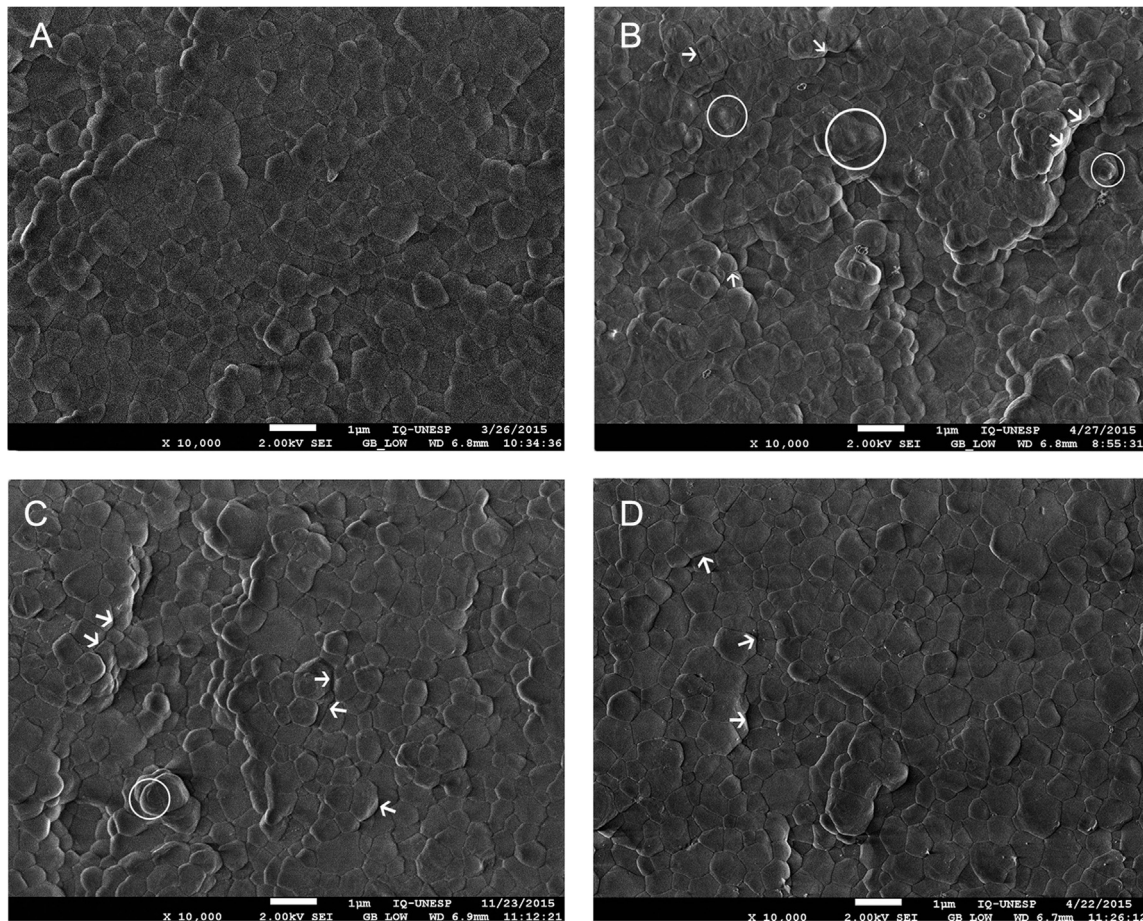


**Fig. 4.** Representative SEM images of infrastructure zirconia (IZr), before and after submission to the different aging processes. (A) Non treated material, (B) Hydrothermal, (C) Mechanical, (D) Hydrothermal & mechanical. Note the elevated grains, empty spaces after treatments. Grain-boundary continuity loss (white arrows), and nucleation and early stage growing zones (delimited with circles). Low gentle-beam mode, 2 kV of acceleration voltage and without any conductive layer.

following equation:

$$P = 1 - \exp \left[ \left( - \frac{\sigma}{\sigma_0} \right)^m \right] \quad (3)$$

where  $P$  is the probability of fracture,  $\sigma$  is the flexural strength,  $\sigma_0$  is the characteristic strength at a fracture probability of 63.21%, and  $m$  is the Weibull modulus, which is the slope of the line plotted on the “ln (ln [1/(1-P)]) vs ln  $\sigma$ ” Cartesian plane.

## 2.5. Surface characterization

Percentages of tetragonal and cubic zirconia crystalline phases were assessed by X-ray diffraction analysis (XRD – Rint 2000, Rigaku, Tokyo, Japan), and calculated according to Garvie and Nicholson’s method [20] modified by Toraya et al. [21]. The instrument parameters were as follows: Cu-K $\alpha$  radiation (40 kV and 70 mA), scan and time range of 20°–90° and 3 continuous seconds, respectively; and a step size of 0.02°. Surface analyses were performed by scanning electron microscopy (JMS-T33A Scanning Microscope, JEOL, MA, USA) in three representative samples for each material and treatment. The following parameters were used: low gentle-beam mode, at 2 kV of acceleration voltage and without any conductive layer. For the mechanical-cycled specimens (groups II and III), the non-contact indenter surface was analyzed because these surfaces were under tensile stress. Additionally, grain size of each material after aging processes were calculated based on planimetric measurements performed on SEM images using computer software (Image Analysis in Java, NIH). At least 100 grains were measured for each material and condition, and two different images

were used.

## 2.6. Statistical analysis

Biaxial fracture values showed a normal distribution according to Kolmogorov–Smirnov tests ( $p < 0.05$ ). A two-way analysis of variance (ANOVA) was applied to determine the treatment influence, followed by Tukey’s multiple comparison test to ascertain significant differences given the aging processes (95% confidence level).

## 3. Results

Two-way ANOVA was significant for material, aging, and interaction between material and aging (Table 2). Irrespective of aging treatment, IZr and PMZ showed higher mean values of biaxial flexural strength (BFS) than AMZ, but the ceramics behaved differently under the aging conditions (Table 3). In IZr and PMZ, the unique significant difference was found between hydrothermal aging and mechanical cycling ( $p = 0.037$ ). For AMZ, there is no difference between the control group and hydrothermal aging ( $p = 0.116$ ), which were significantly different from combined mechanical cycling ( $p < 0.001$ ) and hydrothermal aging ( $p < 0.001$ ). Weibull parameters (Table 4), and plots (Figs. 1–3) revealed that Weibull modulus was lower in hydrothermal aging groups for all studied ceramics, and characteristic strength values were in the same order found in BFS results.

The three aging processes caused superficial modifications in the three materials: elevated grains, several empty spaces, and some impurities appeared. Also grains-boundary continuity was lost, and



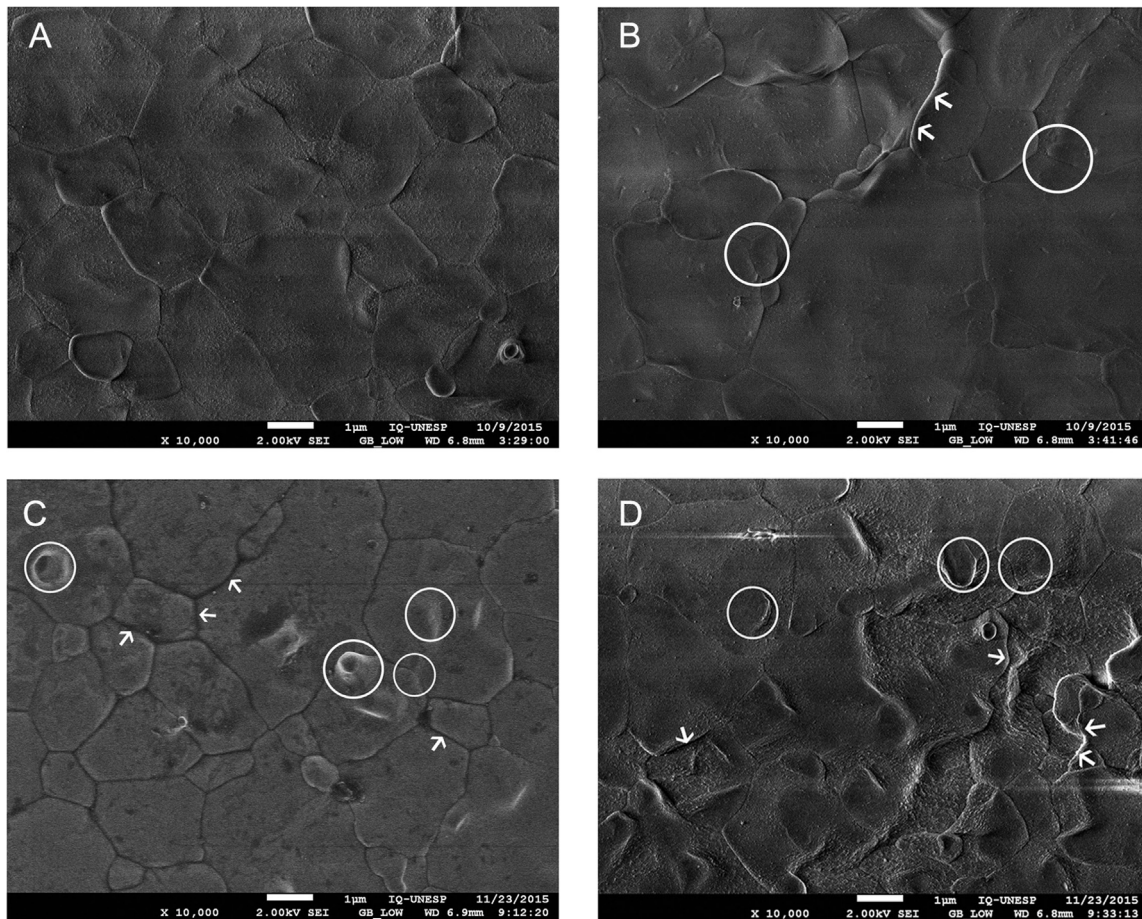


**Fig. 5.** Representative SEM images of anterior monolithic zirconia (AMZ), before and after aging processes. (A) Non treated material, (B) Hydrothermal, (C) Mechanical, (D) Hydrothermal & mechanical. Note elevated grains and empty spaces after treatments. Grain-boundary continuity loss (white arrows), and nucleation and early stage growing zones (delimited with circles). Low gentle-beam mode, 2 kV of acceleration voltage and without any conductive layer.

nucleation and early stage growing zones appeared (see Figs. 4–6).

Table 5 presents the phase analysis by XRD showing monoclinic, tetragonal, and cubic phases after accelerated aging (%). Tetragonal phase is the main part of all the ceramics studied. For IZr and PMZ, monoclinic phase was identified after hydrothermal aging, and after the combination of hydrothermal and mechanical aging. For IZr, cubic phase was found in all conditions, but for PMZ it was only found after hydrothermal aging and the combination of hydrothermal plus mechanical aging. For AMZ, tetragonal and cubic phase was identified in all groups, while monoclinic phase was not found in any condition. Diffraction patterns are included in Fig. 7.

Table 6 shows grain area and perimeter lengths of the materials. Histograms of grain sizes are presented in Fig. 8 for better comprehension.

#### 4. Discussion

The null hypothesis was not accepted, as at least one aging treatment was capable of decreasing the BFS of the studied ceramics. However, the ceramics behaved differently under the aging treatments. While for IZr and PMZ the unique significant difference was found between mechanical cycling and hydrothermal single aging, AMZ was less resistant when mechanical repetitive stress was involved (mechanical cycling and combined hydrothermal plus mechanical cycling).

There is little information about the composition of PMZ and AMZ. According to Sulaiman et al. [22], AMZ has up to 12%  $Y_2O_3$ . The addition of yttria in concentrations higher than 8 mol% produced full crystal cubic stabilization, giving the ceramic higher translucency. AMZ

would be classified as a FSZ (fully stabilized zirconia) due to its yttria content, while IZr and PMZ are classified as PSZ (partially stabilized zirconia). Cubic crystals improve translucency, because of their optical anisotropy and larger grain size, which decrease grain-boundary areas (scattering source). PMZ, in turn, appears to have a similar composition to conventional Y-TZP with 4–6% yttria concentration [22]. On the other hand, FSZ has lower mechanical resistance compared with PSZ, because the cubic phase is unable to undergo monoclinic toughening transformation, as occurs in metastable tetragonal crystals.

Grain growth can be obtained by increasing the maximum temperature in the sintering process [23]. The sintering protocol for AMZ and PMZ was of a maximum temperature of 1600 °C, while for IZr the maximum is 1500 °C. The mean grain size of PMZ ( $0.46 \mu m^2$ ) is 58% larger than IZr ( $0.29 \mu m^2$ ), but AMZ grain size ( $3.96 \mu m^2$ ) is 8.6 times bigger than PMZ grains, and 13.6 times bigger than IZr grains.

XRD analysis shows the co-existence of tetragonal and cubic phase in AMZ and no occurrence of monoclinic phase, even under aging treatments. Indeed, AMZ was stable against hydrothermal aging, in contrast to IZr and PMZ (Table 5). The markedly larger AMZ grain size suggests the presence of cubic phase crystals. This finding is expected for hybrid tetragonal-cubic zirconia, because when cubic grains coexist with tetragonal grains, LTD is accelerated as cubic grains attract yttria from neighboring tetragonal grains, affecting its metastability [24,25]. Hybrid tetragonal-cubic zirconia is more brittle than tetragonal-based due to the size of cubic grains [15]. Y-TZP with cubic phase is unable to have a toughening effect because of reduced tetragonal-to-monoclinic transformation [3,14]. Thus, the lower BFS of AMZ in comparison to IZr and PMZ, mainly after repetitive mechanical stress (mechanical cycling

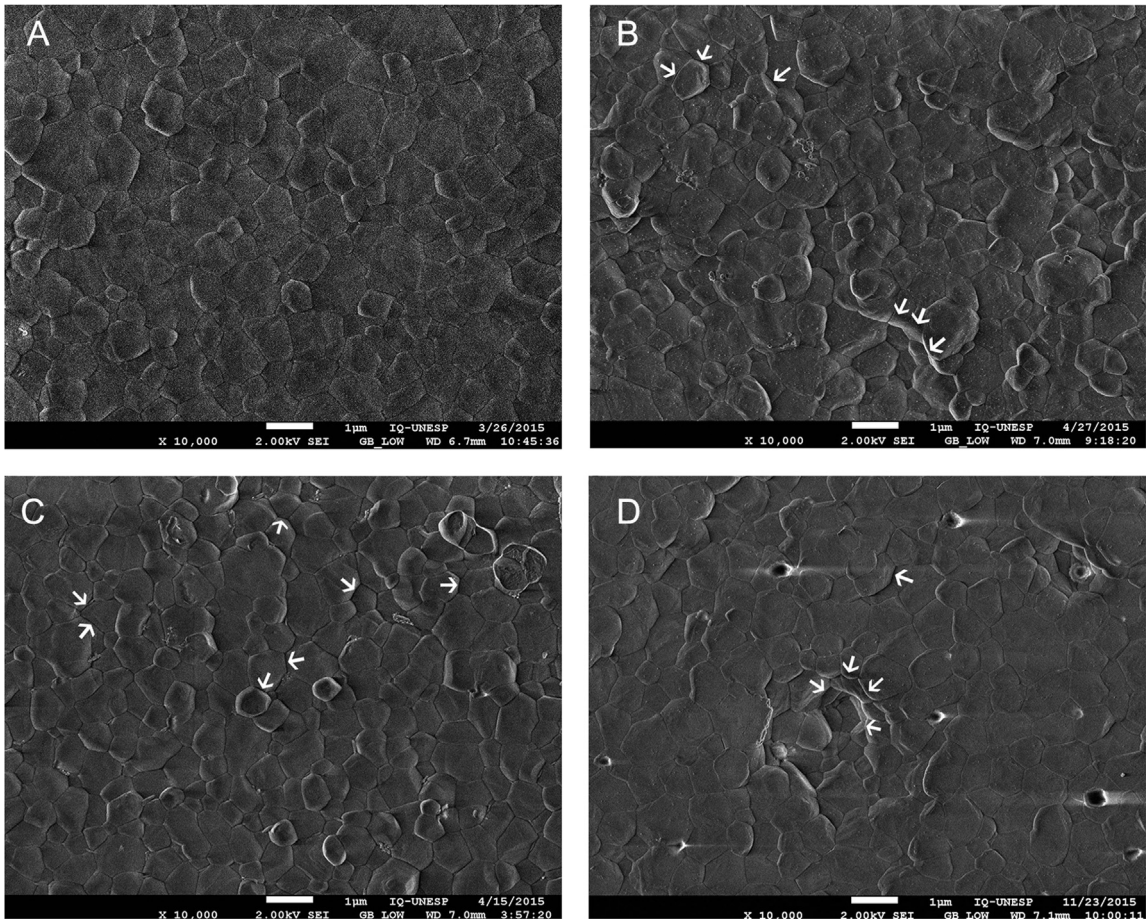


**Fig. 6.** Representative SEM images of and posterior monolithic zirconia (PMZ) before and after aging processes. (A) Non treated material, (B) Hydrothermal, (C) Mechanical, (D) Hydrothermal & mechanical. Note the elevated grains, empty spaces after treatments. Grain-boundary continuity loss (white arrows). Low gentle-beam mode, 2 kV of acceleration voltage and without any conductive layer.

**Table 5**  
Unit cell dimensions and crystalline phase composition percentages after aging processes by X-ray diffraction analyses.

Material	Aging	Tetragonal			Cubic		Monoclinic					Total
		wt%	Unit cell (Å)		wt%	Unit cell (Å)	wt%	Unit cell (Å)				
			α	c				α	α	b	c	
IZr	Control	88.86	3.605	5.177	11.14	5.132	0.00					100.0
	Hydrothermal (H)	64.61	3.605	5.178	10.50	5.133	24.89	5.192	5.254	5.243	99.715	100.0
	Mechanical (M)	88.06	3.604	5.177	11.94	5.130	0.00					100.0
	Combined H & M	54.84	3.603	5.177	20.47	5.135	24.68	5.234	5.120	5.347	99.922	100.0
PMZ	Control	100.00	3.624	5.153	0.00		0.00					100.0
	Hydrothermal	49.91	3.606	5.177	10.38	5.164	39.71	5.168	5.211	5.337	99.057	100.0
	Mechanical	100.00	3.621	5.156	0.00		0.00					100.0
	Combined H & M	58.45	3.603	5.172	11.68	5.174	29.87	5.173	5.207	5.323	99.031	100.0
AMZ	Control	81.04	3.624	5.147	18.96	5.131	0.00					100.0
	Hydrothermal	78.42	3.624	5.148	21.58	5.131	0.00					100.0
	Mechanical	82.31	3.623	5.147	17.69	5.132	0.00					100.0
	Combined H & M	87.16	3.620	5.156	12.84	5.130	0.00					100.0

Quantification of phase content by Garvie and Nicholson’s method [20] modified by Toraya [21].

and hydrothermal aging plus mechanical cycling), is consistent with the large grains observed in SEM images (Figs. 4–6; Table 6), which are likely to be cubic crystals (Table 5). Flexural strength depends on the number of mechanical cycles and load, but there is no current consensus in the literature. Studies have applied from 10,000 cycles up to 5 million of sinusoidal loading, using forces ranging from 20 N to 200 N or 25% of BFS [26–28]. The current study used loads corresponding to 40% of BFS to induce maximum

challenge that allowed specimen survival. Despite the tendency to a slight decrease in BFS of IZr and PMZ after aging by mechanical cycling, XRD analysis did not reveal monoclinic phase in the studied ceramics after mechanical cycling. This may indicate that the stress produced at the specimens’ surface was not capable of inducing tetragonal-to-monoclinic toughening phase transformation to reinforce the materials, or it was not enough to avoid slow crack growth due to the fatigue process. Insignificant percentage of monoclinic phase after mechanical



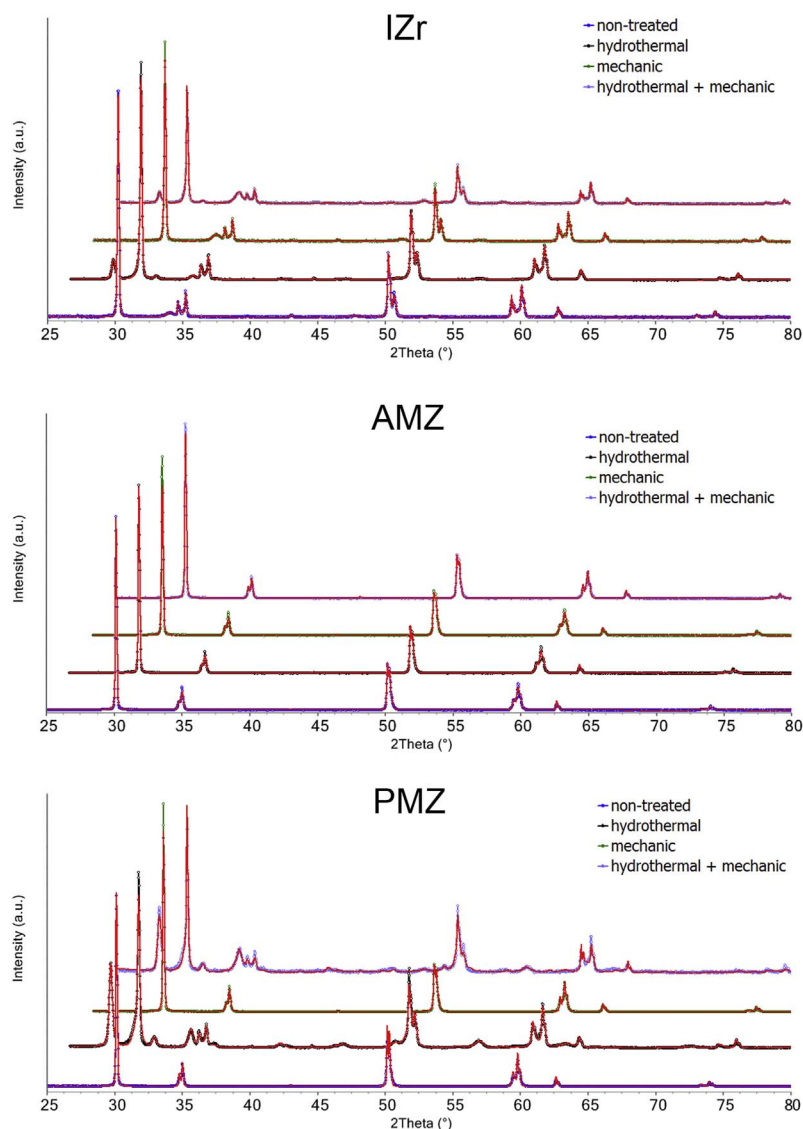


Fig. 7. XRD pattern of infrastructure zirconia (IZr), anterior monolithic zirconia (AMZ) and posterior monolithic zirconia (PMZ) after the various aging treatments comparing non-treated materials.

**Table 6**  
Grain area and perimeter of non-treated materials (mean values).

Material	Area ( $\mu\text{m}^2$ )	Perimeter ( $\mu\text{m}$ )
IZr	0.318	2.13
AMZ	4.877	8.218
PMZ	0.5545	2.762

cycling was observed by Cotes et al. [29], while Pittayachawan et al. [27] did not find monoclinic phase in mechanically-loaded specimens. It is important to point out that non-contact indenter surface of the disc was analyzed, because this face was under tensile stress. Taking into account that XRD identifies crystal phases in the overall sample, XRD may not be able to detect crystalline changes situated in a very small area relative to stress concentration [30]. Moreover, XRD analysis has some limitations, such as an incapacity for detecting transformed fractions smaller than 5% and transformation deeper than the X-ray penetration depth. In other words, the test can detect crystalline changes at a few micrometers below the surface, but cannot analyze bulk transformations [30]. Nevertheless, other methodologies could be useful to complement this phase composition study, especially when a punctual analysis is needed, such as Raman spectroscopy [31], optical interferometry and atomic force microscopy [32].

Regarding simulated LTD, XRD analysis showed a high percentage of monoclinic phase in hydrothermal used alone or when combined with mechanical cycling for IZr and PMZ, but again it was not found in any condition for AMZ. The increase of monoclinic phase induced by hydrothermal aging in conventional Y-TZP, as well as the respective effect on its mechanical properties, is extensively documented in the literature [33]. However, despite some decrease in resistance after hydrothermal treatment being expected, there was no statistical significance found between the control group and hydrothermal aging. Moreover, although there was no significance in terms of statistics, a tendency for a small increase in BFS after single hydrothermal aging treatment for IZr and PMZ was observed. Hydrothermal aging is dependent on the temperature, pressure, time, and thickness of specimen. In addition, tetragonal-to-monoclinic phase transformation is conditional to composition (mainly yttria and aluminum oxide content) and grain size [34,35].

As well as ISO Standard 13356:2008 for implants for surgery, it is recommended that ceramic materials based on yttria-stabilized tetragonal zirconia (Y-TZP) are aged by steam autoclave for 5 h at 0.2 MPa at 134 °C to induce monoclinic phase transformation, but this may not be enough to decrease the ceramics' mechanical properties. In this study, 8 h of hydrothermal aging used alone or in combination with mechanical aging produced, respectively, 24.68% and 24.89% of monoclinic phase percentage in IZr, and 39.71% and 29.87% in PMZ.

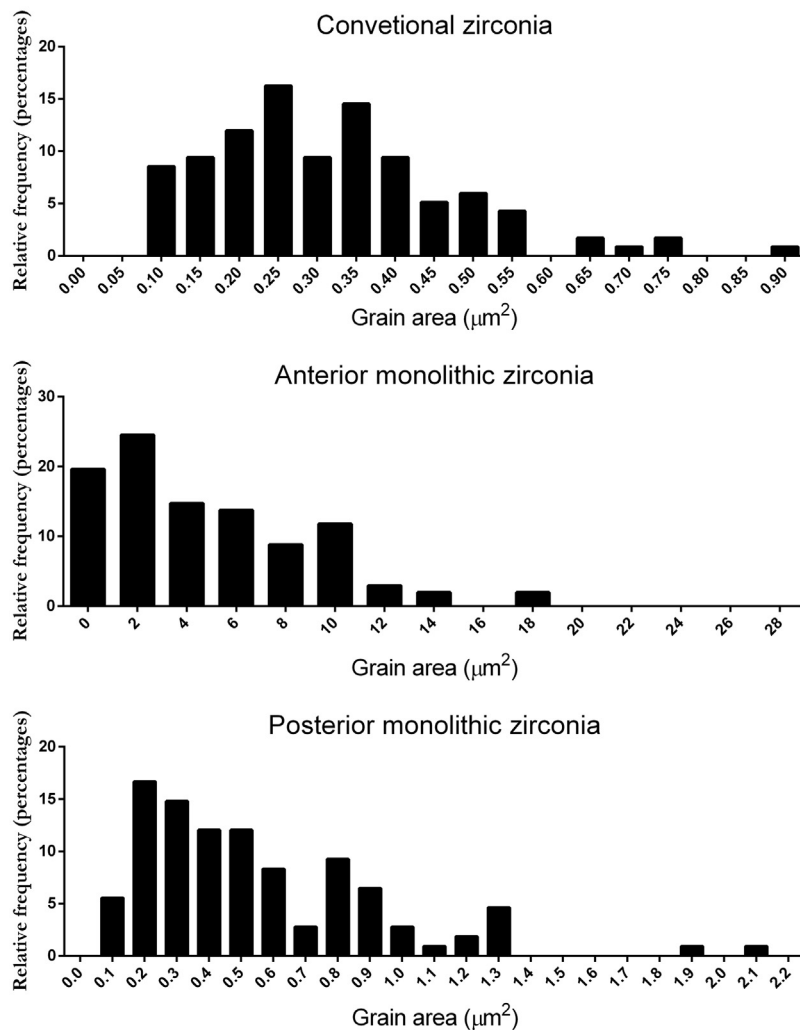


Fig. 8. Histograms of grain sizes of IZr, AMZ, and PMZ.

However, the monoclinic phase concentration identified did not impair the BFS. It has been proven that more aggressive protocols can provoke massive tetragonal-to-monoclinic transformation with evident effects on resistance [36]. The study by Flinn et al. [35] showed rapid transformation in the first 50 h of hydrothermal aging for the monolithic zirconia Prettau, and slow for other materials (Zirprime and Zirtough), reaching more than 70% of monoclinic grains after 200 h of aging. Some specimens spontaneously fractured after those extended periods. It is worth mentioning that the thin bar specimens had 0.2 mm thickness in that study, markedly increasing the aging effects.

XRD showed occurrence of cubic grains in all ceramics, but in PMZ it occurred only in the groups subjected to single hydrothermal aging or combined with mechanical cycling. These results indicate that apart from the expected monoclinic transformation, hydrothermal treatment induced the occurrence of cubic grains. It has been demonstrated that grinding can cause the emergence of cubic grains [27,37] but to the best of the authors' knowledge, there is no study that noticed tetragonal-to-cubic transformations induced by hydrothermal aging.

With regard to reliability study, the lowest value of Weibull modulus ( $m$ ) of hydrothermal aging group of all materials might be related to crystalline phase transformations induced by the treatments. Table 5 shows similar emergence of monoclinic and cubic grains after H and H  $\pm$  M treatments for IZr, but it was found lower " $m$ " just for H treatment. In the case of PMZ there were emergence of crystalline phases, but while cubic grain was found in similar percentage after H and H  $\pm$  M treatments, there was lower concentration of tetragonal phase after H. For AMZ the lowest " $m$ " for H treatment might be related

to higher cubic phase content, and the highest " $m$ " for H  $\pm$  M may be associated to lower cubic phase content. However, the occurrence of these nonhomogeneous phase transformation should be deeply investigated by Micro-Raman and X-ray photoelectron spectroscopy, as stated by Bergamo et al. [38] who also observed lower " $m$ " to zirconia crowns submitted to hydrothermal aging.

In summary, the relationship among composition, microstructure, and sintering procedures to improve optical properties of Y-TZP, and the respective consequences for clinical performance, is a wide and complex issue that needs to be addressed. Thus, it is important to consider the limitations of monolithic translucent Y-TZP before indicating its use.

## 5. Conclusion

Within the limitations of this in vitro study, it can be concluded that AMZ has mean grain size significantly larger than IZr and PMZ, and it is not prone to tetragonal-to-monoclinic transformation. It had lower biaxial flexural strength, and was affected significantly by mechanical cycling. IZr and PMZ showed similar behavior to each other under the aging treatments, showing that their resistance was not affected, other than increasing the monoclinic phase after hydrothermal treatment.

## Acknowledgment

Funding: This work was supported by the Sao Paulo Research Foundation - FAPESP [grant numbers 2013/22539-9 & 2013/21235-6].



## References

- [1] I. Sailer, N.A. Makarov, D.S. Thoma, M. Zwahlen, B.E. Pjetursson, All-ceramic or metal-ceramic tooth-supported fixed dental prostheses (FDPs)? A systematic review of the survival and complication rates. Part I: Single crowns (SCs), *Dent. Mater.* 31 (2015) 603–623, <http://dx.doi.org/10.1016/j.dental.2015.02.011>.
- [2] J. Klimke, M. Trunec, A. Krell, Transparent tetragonal yttria-stabilized zirconia ceramics: influence of scattering caused by birefringence, *J. Am. Ceram. Soc.* 94 (2011) 1850–1858, <http://dx.doi.org/10.1111/j.1551-2916.2010.04322.x>.
- [3] V. Lugh, V. Sergio, Low temperature degradation -aging- of zirconia: a critical review of the relevant aspects in dentistry, *Dent. Mater.* 26 (2010) 807–820, <http://dx.doi.org/10.1016/j.dental.2010.04.006>.
- [4] R.C. Garvie, R.H. Hannink, R.T. Pascoe, Ceramic steel? *Nature* 258 (1975) 703–704, <http://dx.doi.org/10.1038/258703a0>.
- [5] J. Chevalier, C. Olagnon, G. Fantozzi, Subcritical crack propagation in 3Y-TZP ceramics: static and cyclic fatigue, *J. Am. Ceram. Soc.* 82 (1999) 3129–3138, <http://dx.doi.org/10.1111/j.1151-2916.1999.tb02213.x>.
- [6] K. Haraguchi, N. Sugano, T. Nishii, H. Miki, K. Oka, H. Yoshikawa, Phase transformation of a zirconia ceramic head after total hip arthroplasty, *J. Bone Joint Surg.* 83 (2001) 996–1000, <http://dx.doi.org/10.1302/0301-620X.83B7.12122>.
- [7] X. Guo, Property degradation of tetragonal zirconia induced by low-temperature defect reaction with water molecules, *Chem. Mater.* 16 (2004) 3988–3994, <http://dx.doi.org/10.1021/cm040167h>.
- [8] M. Yoshimura, T. Noma, K. Kawabata, S. Somiya, Role of water on the degradation process of Y-TZP, *J. Mater. Sci. Lett.* 6 (1987) 465–467.
- [9] V. Sergio, D.R. Clarke, W. Pompe, Deformation bands in ceria-stabilized tetragonal zirconia/alumina: I, measurement of internal stresses, *J. Am. Ceram. Soc.* 78 (1995) 633–640, <http://dx.doi.org/10.1111/j.1151-2916.1995.tb08224.x>.
- [10] M.J. Lance, E.M. Vogel, L.A. Reith, W.R. Cannon, Low-temperature aging of zirconia ferrules for optical connectors, *J. Am. Ceram. Soc.* 84 (2001) 2731–2733, <http://dx.doi.org/10.1111/j.1151-2916.2001.tb01085.x>.
- [11] B. Basu, J. Vleugels, O. Van Der Biest, Microstructure-toughness-wear relationship of tetragonal zirconia ceramics, *J. Eur. Ceram. Soc.* 24 (2004) 2031–2040, [http://dx.doi.org/10.1016/S0955-2219\(03\)00355-8](http://dx.doi.org/10.1016/S0955-2219(03)00355-8).
- [12] Z. Haibin, L. Zhipeng, K. Byung-Nam, K. Morita, H. Yoshida, K. Hiraga, Y. Sakka, Effect of alumina dopant on transparency of tetragonal zirconia, *J. Nanomater.* (2012), <http://dx.doi.org/10.1155/2012/269064> (5 pp.)–269064 (5).
- [13] U. Anselmi-Tamburini, J.N. Woolman, Z.A. Munir, Transparent nanometric cubic and tetragonal zirconia obtained by high-pressure pulsed electric current sintering, *Adv. Funct. Mater.* 17 (2007) 3267–3273, <http://dx.doi.org/10.1002/adfm.200600959>.
- [14] F. Zhang, K. Vanmeensel, M. Batuk, J. Hadermann, M. Inokoshi, B. Van Meerbeek, I. Naert, J. Vleugels, Highly-translucent, strong and aging-resistant 3Y-TZP ceramics for dental restoration by grain boundary segregation, *Acta Biomater.* 16 (2015) 215–222, <http://dx.doi.org/10.1016/j.actbio.2015.01.037>.
- [15] Y. Zhang, Making yttria-stabilized tetragonal zirconia translucent, *Dent. Mater.* 30 (2014) 1195–1203, <http://dx.doi.org/10.1016/j.dental.2014.08.375>.
- [16] I. Denry, J.R. Kelly, Emerging ceramic-based materials for dentistry, *J. Dent. Res.* 93 (2014) 1235–1242, <http://dx.doi.org/10.1177/0022034514553627>.
- [17] A. Krell, J. Klimke, T. Hutzler, Transparent compact ceramics: inherent physical issues, *Opt. Mater. (Amst.)* 31 (2009) 1144–1150, <http://dx.doi.org/10.1016/j.optmat.2008.12.009>.
- [18] T.A. Sulaiman, A.A. Abdulmajeed, T.E. Donovan, P.K. Vallittu, T.O. Närhi, L.V. Lassila, The effect of staining and vacuum sintering on optical and mechanical properties of partially and fully stabilized monolithic zirconia, *Dent. Mater. J.* 34 (2015) 605–610, <http://dx.doi.org/10.4012/dmj.2015-054>.
- [19] J. Chevalier, B. Cales, J.M. Drouin, Low-Temperature aging of Y-TZP ceramics, *J. Am. Ceram. Soc.* 82 (1999) 2150–2154, <http://dx.doi.org/10.1111/j.1151-2916.1999.tb02055.x>.
- [20] R.C. Garvie, P.S. Nicholson, Phase analysis in zirconia systems, *J. Am. Ceram. Soc.* 55 (1972) 303–305, <http://dx.doi.org/10.1111/j.1151-2916.1972.tb11290.x>.
- [21] H. Toraya, M. Yoshimura, S. Somiya, Calibration curve for quantitative analysis of the monoclinic-Tetragonal ZrO<sub>2</sub> system by X-ray diffraction, *J. Am. Ceram. Soc.* 67 (1984) C119–C121, <http://dx.doi.org/10.1111/j.1151-2916.1984.tb19715.x>.
- [22] T.A. Sulaiman, A.A. Abdulmajeed, K. Shahramian, L. Hupa, T.E. Donovan, P. Vallittu, T.O. Närhi, Impact of gastric acidic challenge on surface topography and optical properties of monolithic zirconia, *Dent. Mater.* 31 (2015) 1445–1452, <http://dx.doi.org/10.1016/j.dental.2015.09.010>.
- [23] B. Stawarczyk, M. Özcan, L. Hallmann, A. Ender, A. Mehl, C.H.F. Hämmerlet, The effect of zirconia sintering temperature on flexural strength, grain size, and contrast ratio, *Clin. Oral Investig.* 17 (2013) 269–274, <http://dx.doi.org/10.1007/s00784-012-0692-6>.
- [24] W.Z. Zhu, Effect of cubic phase on the kinetics of the isothermal tetragonal to monoclinic transformation in ZrO<sub>2</sub>(3mol% Y<sub>2</sub>O<sub>3</sub>) ceramics, *Ceram. Int.* 24 (1998) 35–43, [http://dx.doi.org/10.1016/S0272-8842\(96\)00074-0](http://dx.doi.org/10.1016/S0272-8842(96)00074-0).
- [25] J. Chevalier, S. Deville, E. Munch, R. Jullian, F. Lair, Critical effect of cubic phase on aging in 3mol% yttria-stabilized zirconia ceramics for hip replacement prosthesis, *Biomaterials* 25 (2004) 5539–5545, <http://dx.doi.org/10.1016/j.biomaterials.2004.01.002>.
- [26] H. Yilmaz, S.K. Nemli, C. Aydin, B.T. Bal, T. Tiras, Effect of fatigue on biaxial flexural strength of bilayered porcelain/zirconia (Y-TZP) dental ceramics, *Dent. Mater.* 27 (2011) 786–795, <http://dx.doi.org/10.1016/j.dental.2011.03.019>.
- [27] P. Pittayachawan, A. McDonald, A. Petrie, J.C. Knowles, The biaxial flexural strength and fatigue property of Lava™ Y-TZP dental ceramic, *Dent. Mater.* 23 (2007) 1018–1029, <http://dx.doi.org/10.1016/j.dental.2006.09.003>.
- [28] R.O.A. Souza, L.F. Valandro, R.M. Melo, J.P.B. Machado, M.A. Bottino, M. Özcan, Air-particle abrasion on zirconia ceramic using different protocols: effects on biaxial flexural strength after cyclic loading, phase transformation and surface topography, *J. Mech. Behav. Biomed. Mater.* 26 (2013) 155–163, <http://dx.doi.org/10.1016/j.jmbbm.2013.04.018>.
- [29] C. Cotes, A. Arata, R.M. Melo, M.A. Bottino, J.P.B. Machado, R.O.A. Souza, Effects of aging procedures on the topographic surface, structural stability, and mechanical strength of a ZrO<sub>2</sub>-based dental ceramic, *Dent. Mater.* 30 (2014) e396–e404, <http://dx.doi.org/10.1016/j.dental.2014.08.380>.
- [30] S. Deville, L. Gremillard, J. Chevalier, G. Fantozzi, A critical comparison of methods for the determination of the aging sensitivity in biomedical grade yttria-stabilized zirconia, *J. Biomed. Mater. Res. B Appl. Biomater.* 72 (2005) 239–245, <http://dx.doi.org/10.1002/jbm.b.30123>.
- [31] S.K. Nemli, H. Yilmaz, C. Aydin, B.T. Bal, T. Tiras, Effect of fatigue on fracture toughness and phase transformation of Y-TZP ceramics by X-ray diffraction and Raman spectroscopy, *J. Biomed. Mater. Res. B Appl. Biomater.* 100 (2012) 416–424, <http://dx.doi.org/10.1002/jbm.b.31964>.
- [32] J. Chevalier, L. Gremillard, S. Deville, Low-Temperature degradation of zirconia and implications for biomedical implants, *Annu. Rev. Mater. Res.* 37 (2007) 1–32, <http://dx.doi.org/10.1146/annurev.matsci.37.052506.084250>.
- [33] G.K.R. Pereira, A.B. Venturini, T. Silvestri, K.S. Dapieve, A.F. Montagner, F.Z.M. Soares, L.F. Valandro, Low-temperature degradation of Y-TZP ceramics: a systematic review and meta-analysis, *J. Mech. Behav. Biomed. Mater.* 55 (2015) 151–163, <http://dx.doi.org/10.1016/j.jmbbm.2015.10.017>.
- [34] F. Zhang, K. Vanmeensel, M. Inokoshi, M. Batuk, J. Hadermann, B. Van Meerbeek, I. Naert, J. Vleugels, Critical influence of alumina content on the low temperature degradation of 2–3 mol% yttria-stabilized TZP for dental restorations, *J. Eur. Ceram. Soc.* 35 (2015) 741–750, <http://dx.doi.org/10.1016/j.jeurceramsoc.2014.09.018>.
- [35] B.D. Flinn, A.J. Raigrodski, A. Singh, L.A. Mancl, Effect of hydrothermal degradation on three types of zirconias for dental application, *J. Prosthet. Dent.* 112 (2014) 1377–1384, <http://dx.doi.org/10.1016/j.prosdent.2014.07.015>.
- [36] M. Cattani-Lorente, S.S. Scherrer, P. Ammann, M. Jobin, H.W. Wiskott, Low temperature degradation of a Y-TZP dental ceramic, *Acta Biomater.* 7 (2011) 858–865, <http://dx.doi.org/10.1016/j.actbio.2010.09.020>.
- [37] M. Cattani-Lorente, S. Durual, M. Ameiz-Droz, H.W.A. Wiskott, S.S. Scherrer, Hydrothermal degradation of a 3Y-TZP translucent dental ceramic: a comparison of numerical predictions with experimental data after 2 years of aging, *Dent. Mater.* 32 (2016) 394–402, <http://dx.doi.org/10.1016/j.dental.2015.12.015>.
- [38] E.T.P. Bergamo, W. da Silva, P. Cesar, A.D.B. Cury, Fracture load and phase transformation of monolithic zirconia crowns submitted to different aging protocols, *Oper. Dent.* (2016) 41–43, <http://dx.doi.org/10.2341/15-154-L>.